

Copepod faecal pellet transfer through the meso- and bathypelagic layers in the Southern Ocean in spring

Anna Belcher^{1,2}, Clara Manno³, Peter Ward³, Stephanie Henson¹, Richard Sanders¹, Geraint A. Tarling³

¹National Oceanography Centre, Southampton, SO14 3ZH, UK

²University of Southampton, Southampton, SO14 3ZH, UK

³ British Antarctic Survey, Cambridge, CB3 0ET, UK

Correspondence to: Anna Belcher (A.Belcher@noc.soton.ac.uk)

Abstract. The faecal pellets (FP) of zooplankton can be important vehicles for the transfer of particulate organic carbon (POC) to the deep ocean, often making large contributions to carbon sequestration. However, the routes by which these FP reach the deep ocean have yet to be fully resolved. We address this by comparing estimates of copepod FP production to measurements of copepod FP size, shape and number in the upper mesopelagic (175-205 m) using Marine Snow Catchers, and in the bathypelagic using sediment traps (1,500-2,000 m). The study is focussed on the Scotia Sea, which contains some of the most productive regions in the Southern Ocean, where epipelagic FP production is likely to be high. We found that, although the size distribution of the copepod community suggests that high numbers of small FP are produced in the epipelagic, small FP are rare in the deeper layers, implying that they are not transferred efficiently to depth. Consequently, small FP make only a minor contribution to FP fluxes in the meso- and bathypelagic, particularly in terms of carbon. The dominant FP in the upper mesopelagic were cylindrical and elliptical, while ovoid FP were dominant in the bathypelagic. The change in FP morphology, as well as size distribution, points to the repacking of surface FP in the mesopelagic and in situ production in the lower meso- and bathypelagic, which may be augmented by inputs of FP via zooplankton vertical migrations. The flux of carbon to the deeper layers within the Southern Ocean is therefore strongly modulated by meso- and bathypelagic zooplankton, meaning that the community structure in these zones has a major impact on the efficiency of FP transfer to depth.

1 Introduction

The biological carbon pump (BCP) from the atmosphere to the deep ocean is an important process by which carbon can be sequestered for millennia or longer (Volk and Hoffert, 1985). About 10% of surface ocean primary production sinks out (is exported) of the surface ocean, with the remainder being remineralised in situ. However, only a small fraction of this material (<10%) reaches the deep ocean (Sarmiento and Gruber, 2006), with most of it being respired by grazers or bacteria (Azam et al., 1983) in the upper mesopelagic (Martin et al., 1987). Nevertheless, it is estimated that the BCP keeps atmospheric CO₂ around 200 ppm lower than preindustrial levels (Parekh et al., 2006). Small changes in the BCP, such as a

31 change in the depth at which sinking material is remineralised can result in large changes to the climate system; if the depth
32 at with 63% of sinking carbon is respired is increased by 24 m globally, this could decrease atmospheric CO₂ by 10-27 ppm
33 (Kwon et al., 2009). For this reason, the nature of particles occurring at different depths is important to understand.

34

35 The repackaging of slow-sinking individual phytoplankton cells into fast-sinking faecal pellets (FP) can promote efficient
36 export of POC out of the euphotic zone (Hamm et al., 2001). The contribution of FP to bathypelagic particle fluxes can be
37 large (>90%) (Carroll et al., 1998; Manno et al., 2015; Wilson et al., 2013), providing direct evidence of the importance of
38 zooplankton FP to the transport of carbon to the deep ocean. However, surface produced FP can also undergo intense
39 reworking and fragmentation in the euphotic and upper mesopelagic zones (González et al., 1994b; Wexels-Riser et al.,
40 2001; Wexels Riser et al., 2007), through processes such as coprophagy (ingestion of FP), coprorhexy (fragmentation of FP),
41 microbial remineralisation and physical aggregation and disaggregation (Lampitt et al., 1990; Poulsen and Iversen, 2008;
42 Turner, 2015; Wilson et al., 2008). Thus, FP can also provide a source of nutrition for other zooplankton and bacterial
43 communities *en route* to the deep ocean (Miquel et al., 2015; Wexels-Riser et al., 2001). The complexity of these interacting
44 factors results in a wide range of estimates (<1->100% (Turner, 2015)) of the contribution FP make to POC flux (%FPC),
45 which is typically measured using sediment traps (Dagg et al., 2003; Fowler et al., 1991; Gleiber et al., 2012; Manno et al.,
46 2015; Suzuki et al., 2001; Wassmann et al., 2000; Wilson et al., 2013).

47

48 Differences in FP shape, composition and density, as well as varying depths of production (through zooplankton species
49 residing at different depths and also vertical migration (VM)) will greatly influence the magnitude of FP associated POC that
50 reaches the deep ocean (Atkinson et al., 2012; Steinberg et al., 2000; Wallace et al., 2013; Wilson et al., 2008). Both diel and
51 seasonal migrations of zooplankton can directly transport carbon out of the euphotic zone to the mesopelagic, bypassing the
52 region of rapid remineralisation (Jónasdóttir et al., 2015; Kobari et al., 2008; Steinberg et al., 2000). Different zooplankton
53 feeding strategies will also influence the effect that their vertical migrations have on POC export (Wallace et al., 2013).

54

55 The direct sinking of zooplankton FP can provide an efficient vehicle for the sequestration of carbon in the deep ocean. For
56 example, direct sedimentation of FP from large salp blooms in the upper ocean can result in huge depositions on the sea floor
57 at depths of ~4000 m due to their high sinking velocities (Smith, Jr. et al., 2014). Additionally, the swarming behaviour of
58 krill can result in *en masse* sinking of FP, which can overload recycling zooplankton grazers and be efficiently transferred
59 through the upper ocean (Clarke et al., 1988). Alternatively, FP may arrive in the deep ocean via a FP ‘cascade’ effect
60 (Bodungen et al., 1987; Urrere and Knauer, 1981), being constantly reworked and transformed with depth. The fact that FP
61 have been observed in the deep ocean highlights the important role they play in carbon sequestration, however knowledge of
62 the route by which these FP reach the deep ocean is not yet clear. There is a need for comparisons between the composition
63 and characteristics of sinking FP just below the euphotic zone and in the deep ocean to improve our understanding of both

64 the origin of faecal material reaching the deep ocean and how it is potentially modified by meso- and bathypelagic
65 zooplankton.

66
67 Zooplankton FP can make a large contribution to fluxes of FP in the meso- and bathypelagic of the Scotia Sea (e.g. Belcher
68 et al., 2016b; Cavan et al., 2015; Manno et al., 2015). In this region, the transfer of FP through the mesopelagic (as well as
69 the mechanisms controlling their transfer) is therefore a key determinant of the efficiency of the BCP. Here we use Marine
70 Snow Catchers and deep ocean sediment traps in the Scotia Sea, within the Southern Ocean, to collect intact sinking FP in
71 the upper mesopelagic and bathypelagic respectively, and use these data to compare the characteristics of mesopelagic and
72 bathypelagic FP. We compare copepod abundances in the upper 200 m with FP fluxes in both the upper mesopelagic and
73 bathypelagic in order to understand the processes controlling the fate of FP produced in the epipelagic. We use these data to
74 determine whether FP arriving in sediment traps in the deep ocean are a result of a direct detrital rain from the surface, or are
75 produced in the mesopelagic via the grazing and repackaging of this material by deep zooplankton populations. We focus in
76 particular on copepod FP as copepods are the numerically dominant zooplankton in our study region, typically comprising
77 >90% of total zooplankton (Ward et al., 2012).

78 **2 Methods**

79 **2.1 Study site**

80 Sediment traps have been deployed for a number of years at two sites, P2 and P3 (Figure 1), upstream and downstream of
81 South Georgia (at -55.248 °N, -41.265 °E and -52.812 °N, -39.972 °E respectively) in the Scotia Sea in the Southern Ocean
82 (Manno et al., 2015). The Scotia Sea is mainly located in the eastward flowing Antarctic Circumpolar Current (ACC), which
83 is split by a number of frontal systems including the Southern Antarctic Circumpolar Front (SACCF, Fig. 1). The complex
84 circulation patterns and variability in frontal systems shapes the Scotia Sea ecosystem (Murphy et al., 2007). P3 and P2 are
85 located downstream and upstream of South Georgia respectively, leading to marked differences in community structure with
86 large rapidly sinking diatoms likely to be more prevalent in the iron fertilised downstream region (Korb et al., 2012;
87 Smetacek et al., 2004). Phytoplankton blooms at P3 can be sustained for 3-4 months (Whitehouse et al., 2008), whereas
88 blooms are typically much shorter in the SACCF region where P2 is located (Park et al., 2010), likely influencing the
89 dynamics of the zooplankton community. Variability in regional dispersal or retention by the current systems of the ACC is
90 important for determining the seasonal dynamics of Scotia Sea ecosystems (Murphy et al., 2007; Thorpe et al., 2007).

91
92 During cruises in austral spring 2013 (JR291) and 2014 (JR304) aboard the *RRS James Clark Ross*, samples of sinking
93 particles in the upper mesopelagic were collected using Marine Snow Catchers (MSC) (Table 1) and zooplankton abundance
94 data using Bongo nets. Sediment trap data were obtained from traps deployed in 2012 and 2013 at P2 and P3, at depths of
95 1,500 m and 2,000 m respectively. Mean current velocities in December 2012 and 2013 (measured with a Nortek Aquadopp

96 current meter deployed just below the ST) were 7.2 and 4.5 cm s⁻¹, and, 14.2 and 12.5 cm s⁻¹ at P3 and P2 respectively. These
97 data agree with mean current velocities at the depth of the ST at both sites of <10 cm s⁻¹ observed by Whitehouse et al.,
98 (2012) in 2008, suggesting that the effects of lateral advection are minimal and as such they are not considered in this study.

99 **2.2 Mesozooplankton collection**

100 **2.2.1 Net sampling**

101 Mesozooplankton samples were collected at both P2 and P3 using a motion-compensating Bongo net (61 cm mouth
102 diameter, 2.8 m long, 200 µm mesh). The net was equipped with solid cod ends, deployed to 200 m and hauled vertically to
103 the surface at 0.22 m s⁻¹. Samples were preserved in 4% formalin (w/v) in seawater before being identified to species/taxa
104 using a binocular microscope and staged where appropriate. At least 500 individuals were counted per sample. Counts were
105 converted into ind. m⁻² (0-200 m) based on the area of the Bongo net mouth and the depth of deployment. A total of five
106 deployments were carried out during JR291 and two during JR304. Average abundances for each species/taxa were
107 calculated by averaging all the deployments (from both cruises) at each site. Antarctic krill (*Euphausia superba*) and other
108 large euphausiids were occasionally caught in the Bongo nets, but the Bongo net does not accurately quantify their
109 abundance due to their patchy distribution and net avoidance capabilities. Large euphausiid abundances were therefore not
110 considered, so zooplankton abundances in this study reflect mesozooplankton abundances. In particular, copepod species
111 were overwhelmingly dominant in terms of abundance at our study sites, typically >90% of total zooplankton abundance
112 (Ward et al., 2012). Zooplankton were grouped into; small microcopepod species (*Oithona similis*, *Oncaea sp.* and
113 *Ctenocalanus sp.*) large calanoid copepod species (*Rhincalanus gigas*, *Calanoides acutus*, *Calanus similimus*, *C.*
114 *propinquus*, *Euchaeta spp.*, and *Metridia spp.*), small euphausiids (all euphausiid species caught in net) and other
115 zooplankton (all remaining species).

116 **2.2.2 Prediction of faecal pellet size distribution in epipelagic layers**

117 We predicted the size distribution of FP in the epipelagic layers by using the size distribution of the copepod community
118 assessed via prosome length (PL, mm) (Ward et al. 2012, their table A1) and the known relationship between copepod size
119 and the volume of their FP (FPV, µm³) (Mauchline, 1998; Stamieszkin et al., 2015).

120

$$121 \log_{10} FPV = \theta \log_{10}(PL) + \eta \quad (1)$$

122

123 We take mean values of θ and η of 2.58 and 5.4 respectively from Stamieszkin et al. (2015) derived from literature values of
124 FPV and PL. Using measured copepod abundances, we then calculated the size distribution of FP produced by our
125 population of copepods. We compared the percent abundance in each size class, making the assumption that all copepods
126 were egesting FP at the same rate (see Discussion). As the zooplankton net tows are integrated from the surface to 200 m,

127 there is a slight overlap with the MSC samples, however, as the bulk of zooplankton are found in the upper 100 m (Ward et
128 al., 2014), these net samples are largely representative of the epipelagic layer and we refer to it as such for simplicity. Non-
129 copepod zooplankton (~10 % mesozooplankton abundance) were not considered in this calculation and represent a
130 background error in this approach.

131 **2.3 Faecal pellet collection**

132 **2.3.1 Marine Snow Catcher deployments**

133 Marine Snow Catchers (MSC) were deployed in the upper mesopelagic, defined here as 110 m below the base of the mixed
134 layer depth (MLD) identified from vertical profiles of the water column taken prior to MSC deployments using a
135 Conductivity-Temperature-Depth (CTD) unit (Seabird 9Plus with SBE32 carousel). MSC are large (95 L) PVC closing
136 water bottles, designed to minimise turbulence so particles are more likely to remain intact (Belcher et al., 2016a, 2016b;
137 Cavan et al., 2015; Riley et al., 2012). Once at the appropriate depth, MSC were closed via a mechanical release mechanism,
138 before recovering and leaving on deck for a settling period (2 hours). Following settling, they were drained and particles that
139 sank fast enough to reach the bottom collector tray (“fast sinking” particles (Riley et al., 2012)) were removed from the tray
140 and stored at 2-4°C for further analysis. All particles collected in the MSC tray were counted as it was not necessary to split
141 the sample. Particles reaching the bottom of the tray that were visible by eye were picked from the tray using a wide bore
142 pipette. Given the MSC height of 1.53 m, particles originating at the top of the MSC are required to sink at a minimum rate
143 of 18.4 m d⁻¹ to reach the base of the MSC. However, considering measurements of FP sinking velocity in the Southern
144 Ocean of 27 m d⁻¹ to 1218 m d⁻¹ (Atkinson et al., 2012; Belcher et al., 2016b; Cavan et al., 2015), this is likely sufficient to
145 capture sinking FP.

146 **2.3.2 Sediment trap deployments**

147 Sediment traps (ST) were deployed in the bathypelagic (1500 m to 2000 m). The P3 trap (2,000 m depth) was deployed in
148 May 2013 on cruise JR287, and P2 (1,500 m depth) deployed on 8th December 2012 on cruise JR280. Both traps were
149 recovered in December 2013 on cruise JR291 aboard the *R.R.S. James Clark Ross*. In addition the P2 mooring was
150 redeployed on 7th Dec 2013 and recovered on 28th November 2014 during cruise JR304. Samples from the spring period
151 (October to January) were analysed for comparison with MSC deployments. The ST consisted of a plastic funnel with a
152 baffle at the top (0.5 m² surface area), and a narrow opening at the bottom, through which particles fall into 1 L sampling
153 cups (McClane, PARFLUX Mark 78H-21). The traps were programmed so sampling cups would rotate after 14 to 31 days,
154 with shorter periods set to coincide with expected periods of high productivity. Prior to deployment, each cup was filled with
155 a preservative solution of sodium chloride buffered 0.01% Mercuric Chloride. Upon recovery, samples were photographed
156 and the pH recorded. Swimmers, defined as zooplankton that were alive and intact on entering the trap, were picked out
157 using tweezers and removed from the sample. Each sample was then split into a number of equal aliquots (determined by the

158 amount of material in the sample) using a rotary splitter McClane Wet Sample Divider (WSD-10). Three replicates were
159 analysed for ST FP, with all FP in each replicate counted (see supplementary table S1 for absolute counts). Here we focus on
160 ST trap samples in November and December (austral spring) to match MSC and zooplankton net deployments.

161 **2.4 Faecal pellet analysis**

162 All FP were photographed using an Olympus SZX16 microscope. FP were classified visually as round, ovoid or cylindrical
163 using light microscopy. All FP in each category collected in the MSC were counted, and their length and width measured
164 using ImageJ. For each ST sample, the dimensions of 10-50 FP of each class were measured and, for MSC samples, all FP
165 were counted and measured. FP volumes were calculated for round, ovoid and cylindrical pellets using the formula for a
166 sphere, ellipsoid and cylinder respectively. Equivalent spherical diameters (ESD) were also calculated. We compare FP
167 volume rather than FP number to avoid bias due to possible fragmentation (Wexels Riser et al., 2010). The carbon contents
168 of FP were calculated based on conversion factors of 0.035, 0.052 and 0.030 mg C mm⁻³ for round, ovoid and cylindrical FP
169 respectively based on measurements made on FP collected from the ST in spring-early autumn (Manno et al., 2015).

170

171 Without faecal production experiments of isolated species, it is difficult to ascertain the exact origin of FP collected in the
172 MSC and ST. Previous studies (González, 1992; González et al., 1994a; González and Smetacek, 1994; Martens, 1978;
173 Wilson et al., 2008; Yoon et al., 2001) suggest that ovoid/ellipsoidal pellets originate from copepods, pteropods and
174 larvaceans, cylindrical pellets from krill and copepods, and spherical pellets from amphipods, small copepods and crustacean
175 nauplii.

176 **2.5 Faecal pellet sinking velocities and fluxes**

177 Sinking velocities (w) of a sample of FP collected in MSC were measured on board on both cruises. During JR291, sinking
178 velocities were measured in a graduated glass cylinder in a temperature controlled laboratory (2°C). For each FP, the sinking
179 velocity was calculated from the average of the time taken to sink past two marked distances (10 cm apart), with the starting
180 point more than 10 cm from the water surface. During JR304, sinking velocities were measured in a temperature controlled
181 (at 4°C) flow chamber system (Ploug and Jorgensen, 1999), suspending FP in an upward flow and taking the average of
182 three measurements. Only FP larger than 0.15 mm ESD (i.e. those visible by eye) could be measured. No significant
183 differences were found between sinking velocities measured during JR291 and JR304 by these two different methods
184 (Student's t-test, $p=0.2$).

185 The median sinking velocity of measured FP for each MSC was utilised to calculate the sinking FP flux (FPF).

186

$$187 \quad FPF \text{ (n FP m}^{-2}\text{d}^{-1}\text{)} = \frac{n_{FP}}{A} \times \frac{w}{h} \quad (2)$$

188

189 Here, n_{FP} is the total number of FP collected at the base of the MSC (excluding krill FP), A the area of the MSC opening
190 based on inner MSC diameter, and h the height of the snow catcher (1.53 m).

191 For sediment trap samples, FP fluxes were calculated as follows:

192

$$193 \quad FPF \text{ (} n \text{ FP m}^{-2} \text{d}^{-1}\text{)} = n_{FP}/(A/d), \quad (3)$$

194

195 where d is the number of days that the trap was open (15 days) and A is the area of the sediment trap (0.5 m²).

196 **2.6 Faecal pellet comparisons**

197 FP collected in the ST and MSC were compared in terms of the number of FP in each morphological type as well as in terms
198 of carbon. As the absolute number of FP was vastly different between MSC and ST samples due to attenuation with depth,
199 we compared the percentage abundance and carbon across the size distribution of all FP from measured FP volumes. As only
200 an average FP size for each morphological type (rather than for all individual FP) was measured for samples from the ST
201 deployments, we make use of historical sediment trap data (Manno et al., 2015) at the same sites from December 2009 and
202 2010. The size of all FP in each sample-split were measured in the study of Manno et al. (2015) and hence we use these data
203 to compare size distributions of MSC and ST collected FP. Manno et al. (2015) also categorised FP into ovoid, cylindrical
204 and round, with an additional category of elliptical. We combine cylindrical and elliptical categories due to their similar
205 morphology and to allow comparison with our MSC data. Although this introduces uncertainty in terms of inter-annual
206 variability between 2009-2010 (full sediment trap data) and 2013-2014 (Marine Snow Catcher data), consistency in the FP
207 types and percentages in each category between years (Fig. S2) provides confidence in the use of these historical data.
208 Numbers of large cylindrical FP, probably originating from large euphausiids, were removed from counts given the large
209 potential bias in the quantification of these organisms in the net samples. Again we took into account only the spring data
210 (November and December).

211 **2.7 Statistics**

212 In order to estimate error uncertainty, we take the standard error of our measurements, i.e. multiple Bongo net tows for
213 zooplankton, multiple MSC deployments for mesopelagic FP, and multiple ST deployments for bathypelagic FP. We
214 compare zooplankton size distributions using a Kolmogorov-Smirnov test. FP size distributions (in terms of % abundance)
215 are also compared using an Anderson-Darling k-sample test as this test is more sensitive to differences in the tails and
216 differences in shift, scale and symmetry when means are similar (Engmann and Cousineau, 2011). All statistics were carried
217 out in RStudio (version 0.98.1091; R development core team, 2014).

218 **3. RESULTS**

219 **3.1 Zooplankton community and faecal pellet production**

220 On average, total zooplankton abundances and species compositions were similar at P2 and P3 (Figure 2), with small
221 microcopepod species *Oithona similis*, *Oncaea sp.* and *Ctenocalanus sp.* outnumbering the main large calanoid copepod
222 species (*Rhincalanus gigas*, *Calanoides acutus*, *Calanus similimus*, *C. propinquus*, *Euchaeta spp.*, and *Metridia spp*) (Table
223 S1, Figure 2). The number of zooplankton with PL <2 mm was similar at P2 and P3 (ratio P3:P2 of 1.1), but the abundance
224 of larger copepods (4-7 mm PL) at P3 was almost double that of P2 (ratio P3:P2 of 1.8) (Fig. S1).

225
226 The predicted size distribution of egested FP from our mesozooplankton copepod community highlights that most FP
227 egested in the epipelagic would be in the smallest size category <0.001 mm³ (97.6 ± 20.3% and 97.0 ± 4.0% at P2 and P3
228 respectively) with low contributions (<2%) from each of the larger FP size categories (Fig. 3a). The high standard error of
229 FP <0.001 mm³ at P2 is in part due to very high abundances of *Oithona similis* during one deployment. Removing this net
230 from the average gives 97.8±13.7% FP<0.001 mm³. The predicted size distributions of FP at P2 and P3 were not
231 significantly different ($p>0.5$, Mann-Whitney U-test, Kolmogorov-Smirnov test, and Anderson-Darling k-sample test).

232 **3.2 Sinking faecal pellets**

233 Sinking faecal pellets collected by the MSC (upper mesopelagic) and the ST (bathypelagic) are described in terms of size
234 and shape to assess changes between these two layers.

235 **3.2.1 Faecal pellet shape**

236 The morphologies of FP captured by the MSC at P2 were heterogeneous (Fig. 4, Figure 5a), with cylindrical/elliptical FP,
237 and round FP making up similarly high percent contributions to the total number of FP. Conversely, a single morphology
238 dominated in the P3 MSC samples which were cylindrical FP of <0.005 mm³ (Figure 5c).

239
240 All morphological classes found in the upper mesopelagic (MSC samples) were also present in the bathypelagic (ST
241 samples, Figure 4). However, the dominant type of FP changed between these two layers (Figure 5). Ovoid FP made only
242 low contributions (<8.3% and <1.4% at P2 and P3 respectively) to total FP abundance in the MSC samples but were the
243 dominant type in most size categories in the ST samples (up to 25.2% and 13.1% at P2 and P3 respectively, Figure 5).

244 **3.2.2 Faecal pellet size**

245 The predicted FP size distributions of pellets produced in the epipelagic by the net caught copepod community were
246 significantly different to those observed in the upper mesopelagic (MSC samples) at both P2 and P3 (Kolmogorov-Smirnov

247 test, $D=0.58$ (P2), $D=0.67$ (P3), $DF=11$, $p<0.01$). Comparison of Figure 3a and b reveals that there was a reduced dominance
248 of the smallest FP ($0-0.001 \text{ mm}^3$) from $>96 \pm <20\%$ to $<18 \pm <5\%$ between the two layers at both sites.

249

250 A further loss in the smaller FP size categories is apparent between the upper mesopelagic MSC samples and the
251 bathypelagic ST samples (Fig. 3c). FP $<0.003 \text{ mm}^3$ in volume decreased from $35.5 \pm 13.4\%$ to $5.0 \pm 0.4\%$ at P2 and from
252 $52.3 \pm 6.7\%$ to $14.0 \pm 5.7\%$ at P3. Based on size alone, the FP community appears to have become less diverse in the
253 bathypelagic layer, with most FP ($>80\%$) occupying a narrower size range in the ST samples, ($0.003-0.01 \text{ mm}^3$) compared
254 to the MSC samples ($0.001-0.02 \text{ mm}^3$). FP size distributions in the MSC and ST were not however significantly different at
255 either P2 or P3 (Anderson-Darling k-sample test, $T.AD=1.3$, $DF=11$, $p=0.2$ and $T.AD=0.43$, $DF=11$, $p=0.9$ at P2 and P3
256 respectively). Re-running the test for only FP size categories $<0.003 \text{ mm}^3$ highlights a significant difference in the %FP
257 abundance in the smaller size categories between the MSC and ST ($p=0.03$ at both P2 and P3).

258 **3.3 Faecal pellet carbon**

259 Although small FP were numerically dominant in the MSC, comparison of Figure 5 and Figure 6 reveals higher
260 contributions of the larger FP size classes to total FP carbon (FPC). This is not unexpected as larger FP contain a larger
261 amount of carbon. FPC data highlight the importance of the loss of large FP to the carbon sinking through the water column.
262 Although abundances of small FP greatly reduced with depth, this does not represent such a large change in terms of carbon.

263 **3.4 Faecal pellet sinking velocities and fluxes**

264 Sinking velocities of FP (excluding krill FP) collected in the MSC ranged from 52 to 382 m d^{-1} at P2 and 13 to 227 m d^{-1} at
265 P3, reflecting the range in FP shapes and sizes. Generally small FP had lower sinking velocities than larger FP. We measured
266 FP sinking rates (excluding krill FP) of $47-120 \text{ m d}^{-1}$ for FP $<0.002 \text{ mm}^3$, and $36-270 \text{ m d}^{-1}$ for FP $>0.02 \text{ mm}^3$ (supplementary
267 table S2). Rates measured in this study are consistent with the range of $5-220 \text{ m d}^{-1}$ given by Turner,(2002) for copepod FP.

268

269 At P3, the flux of cylindrical and elliptical FP in the MSC was an order of magnitude higher than fluxes of round or ovoid
270 FP ($190,716 \text{ FP m}^{-2} \text{ d}^{-1}$ compared to $32,172 \text{ FP m}^{-2} \text{ d}^{-1}$). Similarly at P2, cylindrical and elliptical FP were the dominant FP
271 type ($21,128 \text{ FP m}^{-2} \text{ d}^{-1}$), but fluxes of round FP were also important ($14,596 \text{ FP m}^{-2} \text{ d}^{-1}$) at this site (Table 2). FP fluxes in
272 the ST were dominated by ovoid FP at both sites (Table 2).

273 **4. DISCUSSION**

274 In this study we compare predicted size distributions of FP produced by the copepod community in the epipelagic, to those
275 of sinking FP in the upper mesopelagic (from MSC) and the bathypelagic (from ST) in order to determine the fate of FP

276 sinking through the mesopelagic and assess the importance of deep dwelling zooplankton on the efficiency of the BCP in the
277 Southern Ocean.

278 **4.1 Changes in faecal pellet with depth: upper mesopelagic**

279 Our data suggest that small FP are not transferred efficiently from the epipelagic to the meso- and bathypelagic, and hence
280 make a small contribution to FP fluxes at depth, particularly in terms of carbon. Comparison of estimated copepod FP
281 production with measurements of sinking FP in the upper mesopelagic (from MSC) gives an indication of the degree of
282 retention in that layer. The community at both P2 and P3 was dominated by microcopepod species which, based on their
283 size, produce small FP which are expected to sink more slowly than large FP (Komar et al., 1981; Small et al., 1979;
284 Stamieszkin et al., 2015). Agreeing with the data presented here, small FP ($<0.002 \text{ mm}^3$) are predicted to have a sinking
285 velocity three times slower than larger FP ($>0.02 \text{ mm}^3$) based on the empirical relationship of Small et al. (1979) for copepod
286 FP.

287
288 The longer residence time of small FP in the upper ocean (due to their slower sinking velocities) means they are exposed to
289 remineralisation processes such as coprophagous feeding, fragmentation and microbial remineralisation, for a longer period
290 of time. This type of retention filter and low export efficiency of small FP has been observed in a number of oceanographic
291 environments (e.g. Dagg et al., 2003; Viitasalo et al., 1999; Wexels-Riser et al., 2001). Wexels Riser et al. (2010) made
292 observations over the upper 200 m of a Norwegian fjord, finding that large FP produced by *Calanus finmarchicus*
293 contributed disproportionately to vertical flux despite large numbers of small FP produced by *Oithona similis*, agreeing well
294 with the loss of small FP that we observed in the Scotia Sea.

295
296 It is important to acknowledge here, that although the 200 μm mesh used in this study is commonly used in zooplankton
297 surveys, this leads to an underestimation of the smaller zooplankton size classes present in the epipelagic. Ward et al., (2012)
298 found that a 53 μm mesh caught 5.87 times more zooplankton than a 200 μm net in the upper mesopelagic of the northern
299 Scotia Sea in spring. However, in this study an underestimation of the small zooplankton size classes serves to reinforce the
300 fact that small FP dominate the flux of FP out of the epipelagic and are largely attenuated as they pass through the
301 mesopelagic.

302
303 Comparison of freshly egested FP size distributions with the size distributions of FP sinking through the mesopelagic relies
304 here on the assumption that different species within the copepod community had the same rates of egestion. FP production
305 varies with species, as well as factors such as season and food availability; the range in FP production rates between different
306 copepod species across a number of high latitude studies is 2-48 FP ind.d⁻¹ (Dagg et al., 2003; Daly, 1997; Roy et al., 2000;
307 Thibault et al., 1999; Urban-Rich et al., 1999). However, as the estimated abundance of egested FP in the smallest size
308 category (0-0.001 mm^3) is between 60-250 times greater than the next largest category, the smallest FP are still likely to

309 dominate the FP community even if egestion rates are varied within reasonable bounds. Therefore, despite our assumptions
310 regarding rates of egestion, our conclusion of rapid attenuation of these small FP in the upper mesopelagic remains valid.

311 **4.2 Changes in faecal pellet with depth: meso- to bathypelagic**

312 Our data reveal a change in FP size, shape and abundance between the upper mesopelagic and bathypelagic of the Scotia Sea
313 suggesting in situ FP production by deeper dwelling zooplankton. The occurrence of intact and fresh FP in deep sediment
314 traps in the Southern Ocean (e.g. Accornero et al., 2003; Manno et al., 2015) may therefore be a result of an indirect,
315 cascade-like transfer through the mesopelagic as they are reprocessed by different zooplankton communities (Miquel et al.,
316 2015; Urrere and Knauer, 1981).

317
318 Urrere and Knauer (1981) deployed free-floating traps off the Monterey Peninsula in California. They observed a decrease in
319 numerical FP fluxes in the upper 500 m, but FP fluxes increased by a factor of 2.7 from 500 m to 1500 m. This increase was
320 largely due to elliptical FP, suggesting the presence of deep resident (or overwintering) zooplankton populations (Urrere and
321 Knauer, 1981). The authors conclude that organic material reaches the deep ocean (supporting deep resident zooplankton
322 populations) through in situ repackaging of detritus and via heterotrophy as well as inputs from migrating populations,
323 emulating the “ladder of migrations” first proposed by Vinogradov (1962). More recently, Miquel et al. (2015) deployed
324 drifting sediment traps in the upper 210 m of the Beaufort Sea, observing increases in elliptical FP with depth and decreases
325 in cylindrical FP. They explain this by the presence of omnivorous and carnivorous zooplankton in the mesopelagic, whose
326 primary food sources are the vertical flux of organic matter and other organisms. In agreement with our observations, Suzuki
327 et al. (2003) observed large declines in cylindrical FP between sediment traps deployed at 537 and 796 m in the marginal ice
328 zone of Antarctica, and increases in elliptical FP over the same depth range. They suggest that coprophagous feeding and
329 new FP production can explain some of the loss of cylindrical FP, with fragmentation into small sinking particles explaining
330 the rest. As different zooplankton species produce different shapes of FP, a change in FP shape can suggest a change in
331 zooplankton community structure.

332
333 At both P2 and P3 we saw an increase in the contribution of ovoid FP to the total number of FP between the upper
334 mesopelagic (MSC samples) and bathypelagic (ST samples), increasing by factors of 4.5 and 8.5 at P2 and P3 respectively.
335 This suggests that there is either an input of ovoid FP at depth, or that cylindrical-elliptical and round FP are preferentially
336 remineralised in the mesopelagic. We made both size and shape measurements of FP in the upper mesopelagic and
337 bathypelagic, allowing us to discern if there is indeed production of new ovoid FP at depth. At both P2 and P3, we observed
338 size classes of ovoid FP in the ST (0.003-0.008 mm³) that were not present in the MSC, which rules out selective
339 remineralisation. Furthermore, the intact shape of ovoid FP in the ST argues against fragmentation as a cause of this change
340 in size distribution. In agreement with Manno et al. (2015), we observed that ovoid FP in the ST showed fewer signs of
341 fragmentation and were more intact than cylindrical or elliptical FP at both P2 and P3. Estimates of FPC in ST samples

342 indicates that these ovoid FP also make a large contribution to the flux of POC and, as such, their production at depth
343 represents a mechanism for long term storage of carbon in the ocean. Hence, we conclude that FP fluxes to depth are
344 augmented by FP produced in situ at depth.

345
346 We can estimate the size class of zooplankton producing the FP we find at depth based on the FP size class and Equation 1.
347 We estimate that zooplankton of PL 2.6-3.8 mm and 2.6-3.2 mm could have produced the FP we observed in the ST, based
348 on dominant size classes of FP of 0.003-0.008 mm³ and 0.003-0.005 mm³ at P3 and P2 respectively. Of the species within
349 these size classes recorded in the Bongo net tows at P2 and P3, *Calanoides acutus IV* and *Metridia gerlachei* adults were the
350 most abundant and may be responsible for the flux of these FP to the ST. *C.acutus* is a known seasonal migrator in the
351 region, occurring in the upper 200 m in summer but residing deeper (~200-600 m) in spring (Ward et al., 2012). *Metridia*
352 *spp.* are also known migrators (Ward et al., 1995, 2006b; Ward and Shreeve, 1999), found to be one of the more abundant
353 species in the 500-1000 m depth range based on *Discovery Investigations* to the west of the Drake Passage (Ward et al.,
354 2014). Ward et al. (2014) find the most abundant species in this depth range to be *Oncaea spp.*, *Oithona frigida* and
355 *Microcalanus pygmaeus*, all of which are too small (≤ 0.5 mm PL) to produce the larger FP that were dominant in the ST.
356 Similar to the situation in the epipelagic and upper mesopelagic, we suggest that although small species are more abundant,
357 they produce small FP which sink slowly and are rapidly remineralised. It is likely that it is the less abundant larger
358 carnivores and recyclers in the lower mesopelagic that are contributing more to the flux of carbon to the deep ocean through
359 the production of large FP, agreeing with the modelling study of Stamieszkin et al., (2015). Calanoid copepod families
360 *Aetideidae*, *Heterorhabdidae*, *Metridinidae* and *Euchaetidae* are also common in the mesopelagic of the Scotia Sea and
361 surrounding area (Laakmann et al., 2009; Ward et al., 1995; Ward and Shreeve, 1999), and are of an appropriate size (as
362 adults or other copepodite stages) to produce the larger FP that were dominant in the ST. Although we can only speculate as
363 to the possible producers of FP in the ST, it is clear that appropriately sized zooplankton are sufficiently abundant in the
364 mesopelagic to influence the flux of FP to the ST.

365
366 When comparing datasets collected via different methods (in this case Bongo nets, MSC and ST), it is important to consider
367 the different time and space scales over which they measure. The zooplankton Bongo net samples integrated vertically over
368 the top 200 m and temporally over the period over which replicate samples were taken (a few days at each site for both
369 cruises). MSC samples were an instantaneous snapshot of the particle flux and, at a deployment depth of 110 m below the
370 mixed layer, they integrate over spatial scales of tens of kilometres (based on median sinking rates at P2 and P3 and a current
371 speed of 10 cm s⁻¹). Conversely, ST samples captured the flux over a 15 day period and at a deployment depth of 1500 and
372 2000 m had a potential sample collection area on spatial scales of hundreds of kilometres (based on the same conditions). If
373 zooplankton communities vary significantly over tens of kilometres then this would reduce the direct comparability of MSC
374 and ST data. Previous studies in the region suggest that much of the Scotia Sea is populated by a single zooplankton
375 'community', but there are regional differences in the stage of phenological development. (Ward et al., 2006a), implying that

376 the species composition may not vary on short spatial scales. Changes in the species stage are likely tied to changes in
377 phytoplankton productivity, as for much of the time, Southern Ocean zooplankton are food limited (Ward et al., 2006a).
378 Cluster analysis of phytoplankton in the Scotia Sea reveals distinct communities (in terms of abundance, community
379 structure and productivity) on spatial scales of hundreds of kilometres (Korb et al., 2012), and hence we would not expect
380 significant changes in the stage-structure of zooplankton on the spatial resolution of the MSC, making these results more
381 comparable to those of the ST. The high sinking rates of zooplankton FP means that their occurrence in ST is representative
382 of the conditions directly above the ST (Buesseler et al., 2007). Slow-sinking particles spread out more as they sink which
383 increases our uncertainty in depth comparisons of smaller FP. However, the spatial scale of zooplankton variability at our
384 study site means that slow-sinking FP particles reaching the ST likely reflect the same zooplankton community structure as
385 occurring directly above the ST. For each of our three methods (nets, MSC and ST), we take averages over multiple years
386 which should also reduce the uncertainties associated with the various spatial and temporal resolutions of the three methods.
387 However, we acknowledge that the different spatial and temporal scales of measurement could also contribute to some of the
388 vertical changes in FP shape and size structure that we observed.

389

390 **4.3 Role of meso- and bathypelagic zooplankton**

391 Our data suggest that zooplankton residing below the euphotic layer repackage sinking detritus and produce FP which are
392 able to pass through the lower mesopelagic and be collected in ST in the bathypelagic. Observations made at P2 and P3 in
393 autumn show that, during the night, the highest zooplankton abundances are in the upper 125 m (C.Liszka pers. comm.).
394 However corresponding daytime surface abundances are typically lower which may be partially explained by certain species
395 that migrate vertically in the water column (C.Liszka pers. comm.). We suggest that diel vertical migrators may contribute to
396 the relatively fresh FP we found at depth. A modelling study by Wallace et al. (2013) suggests that FP penetrate deeper in
397 the water column when there is zooplankton vertical migration, with the deepest FP production occurring when zooplankton
398 undertake diel vertical migrations rather than foray type feeding (multiple ascents and descents during a day). Resident
399 zooplankton populations were observed below 150 m depth, with a peak at 375-500 m, most notably at P3 (C.Liszka
400 pers.comm.), suggesting that the deeper parts of the community, consisting of non-migrators or seasonal or ontogenetic
401 migrators are also important at our study site and could repackage organic material in the upper mesopelagic, and may have
402 produced some of the intact FP which we observed in our ST.

403

404 The abundance of zooplankton typically declines rapidly over the upper 1000 m of the water column (Ward et al., 1995,
405 2014; Ward and Shreeve, 1999), suggesting that any new FP production below the depth of our MSC samples is likely to
406 take place in the upper to mid mesopelagic where zooplankton abundances are higher. Zooplankton are more concentrated in
407 the epipelagic, however, the total abundance of zooplankton in the meso- and bathypelagic can be high due to the large depth
408 extent of these layers. In the Antarctic Zone (to the west of our study site), Ward et al. (2014) found that the total depth

409 integrated zooplankton abundance in the 250-2000 m horizon (extrapolating abundances recorded at 750-1000 m down to
410 2000 m) is about three quarters (0.74) of the zooplankton abundance in the top 250 m. Therefore it is likely that there is still
411 substantial production of FP in the lower mesopelagic, and compared to FP produced in the epipelagic, FP produced in the
412 lower mesopelagic are subject to remineralisation processes over a shorter distance, so are more likely to reach the deep
413 ocean intact.

414
415 Despite the similarities in copepod abundances at P2 and P3, the numbers of FP collected at P3 were an order of magnitude
416 higher than at P2. Surface phytoplankton productivity at P3 is typically much higher than at P2, with large blooms occurring
417 in most years (Borrione and Schlitzer, 2013; Korb et al., 2008, 2012). This may in part explain higher FP fluxes at the P3
418 site, as in good feeding conditions (such as those measured during JR304 (Belcher et al., 2016b)) FP production rates have
419 been shown to be higher (Besiktepe and Dam, 2002; Butler and Dam, 1994). The zooplankton community structure may also
420 affect the fate of FP in the mesopelagic. Previous studies have found relationships between POC export and the presence of
421 microcopepod species, suggesting that low POC export may be attributed to coprophagy and/or coprorhexy (Suzuki et al.,
422 2003; Svensen and Nejstgaard, 2003). More recently, several studies have proposed that the main role of small zooplankton
423 species may be to fragment FP rather than ingest them (Iversen and Poulsen, 2007; Poulsen and Kiørboe, 2005; Reigstad et
424 al., 2005). Regardless of the mechanism, previous studies agree that high microcopepod abundances can lead to increased FP
425 retention. The ratio of small copepods to large calanoids is higher at P2 (Fig. 2), which may result in greater losses of FP in
426 the epi- and mesopelagic, resulting in lower numbers of FP captured in our MSC and ST at P2. Indeed, we see higher
427 attenuation of FP fluxes at P2 than P3 between our measurement depths (Table 2).

428
429 The flux of FP reaching the deep ocean therefore depends not only on surface production, but also on the meso- and
430 bathypelagic zooplankton populations and the balance between FP retention and FP production. Our data implies that in situ
431 FP production in the mesopelagic accounted for additional fluxes of FP to the bathypelagic at both P2 and P3. However as
432 there is the potential for further working, fragmentation and remineralisation of FP produced in the mesopelagic, the gross
433 deep FP production cannot be quantified here. We therefore cannot determine whether higher FP fluxes at P3 are due
434 primarily to reduced FP attenuation or to increased FP production at depth; most likely a combination of both mechanisms is
435 taking place. Previous work in the region, has however found that in the upper mesopelagic (mixed layer depth-200 m) FP
436 attenuation is higher at P2 than P3 (Belcher et al., 2016b).

437
438 Our comparison of FP size, shape and abundance in the upper mesopelagic and lower bathypelagic agrees with previous
439 hypotheses (Accornero et al., 2003; Manno et al., 2015; Suzuki et al., 2003), that in situ FP production augments the flux of
440 FP to depth in the Southern Ocean. We find that the occurrence of intact FP in deep ST could be explained by both vertical
441 migrations of zooplankton, and repackaging and in situ FP production by meso- and bathypelagic zooplankton populations
442 (Figure 7). Taking an integrated surface production of $1 \text{ g C m}^{-2} \text{ d}^{-1}$ (based on measurements by Korb et al. (2012) to the

443 northwest of South Georgia), and assuming an assimilation efficiency of 66% (Anderson and Tang, 2010; Head, 1992)
444 during vertical migration (left panel Fig. 7, Scenario 1), we calculate that up to $340 \text{ mg C m}^{-2} \text{ d}^{-1}$ could reach the depth of
445 migration (this depth will vary both between species and seasonally). In comparison, if FP are repackaged multiple times on
446 their transit through the mesopelagic then FP will be assimilated multiple times, resulting in reduced transfer of carbon when
447 compared to diel vertical migration. For example, FP that are assimilated twice over the same vertical distance as a typical
448 vertical migration (right panel, Fig. 7, Scenario 2), result in up to $115 \text{ mg C m}^{-2} \text{ d}^{-1}$ reaching the same depth. The exact
449 difference in carbon transfer between these two routes (Scenario 1 and 2) will depend on the number of repackaging steps
450 over the migration depth, specific assimilation efficiencies of the repackaging copepods as well as loss of FP carbon via
451 remineralisation. However, these calculations highlight that the route by which the FP are transferred to depth is a key
452 control on the amount of carbon reaching depth. Regardless of the feeding mode of these mesopelagic zooplankton
453 communities (detritivory, omnivory or carnivory), production of FP at depth via both the aforementioned scenarios supports
454 the transfer of intact FP to the deep ocean, supporting the sequestration of carbon on long timescales. There is therefore a
455 need to link meso- and bathypelagic zooplankton communities (particularly the larger size classes) to carbon fluxes within
456 global biogeochemical models by refining the contribution of different zooplankton size classes to carbon fluxes via their
457 differential FP production rates and sinking speed.

458

459 **Acknowledgements**

460 We would like to thank the crew, officers and scientists aboard the *R.R.S. James Clark Ross* during research cruises JR291
461 and JR304. Particular thanks to Elena Ceballos Romero, Fred le Moigne, Andy Richardson, and Manon Duret for their
462 invaluable help with marine snow catcher deployments. Thanks to Cecilia Liszka for providing information on the deep
463 mesozooplankton community at our study site. Fieldwork was supported by a NERC AFI Collaborative Gearing Scheme
464 grant to Stephanie Henson. Geraint A. Tarling and Clara Manno were supported by the Ocean Ecosystems programme at
465 British Antarctic Survey.

466

467 **References**

468 Accornero, A., Manno, C., Esposito, F. and Gambi, M. C.: The vertical flux of particulate matter in the polynya of Terra
469 Nova Bay . Part II . Biological components, *Antarct. Sci.*, 15(2), 175–188, doi:10.1017/S0954102003001214, 2003.
470 Anderson, T. R. and Tang, K. W.: Carbon cycling and POC turnover in the mesopelagic zone of the ocean : Insights from a
471 simple model, *Deep. Res. Part II*, 57(16), 1581–1592, doi:10.1016/j.dsr2.2010.02.024, 2010.
472 Atkinson, A., Schmidt, K., Fielding, S., Kawaguchi, S. and Geissler, P. A.: Variable food absorption by Antarctic krill:
473 Relationships between diet, egestion rate and the composition and sinking rates of their fecal pellets, *Deep Sea Res. Part II*
474 *Top. Stud. Oceanogr.*, 59–60, 147–158, doi:10.1016/j.dsr2.2011.06.008, 2012.

475 Azam, F., Frenchel, T., Field, J. G., Gray, J. S., Meyer-Reil, L. A. and Thingstad, F.: The ecological role of water-column
476 microbes in the sea, *Mar. Ecol. Prog. Ser.*, 10, 257–263, doi:10.3354/meps010257, 1983.

477 Belcher, A., Iversen, M., Giering, S., Riou, V., Henson, S. and Sanders, R.: Depth-resolved particle associated microbial
478 respiration in the northeast Atlantic, *Biogeosciences*, 13, 4927–4943, doi:10.5194/bg-2016-130, 2016a.

479 Belcher, A., Iversen, M. H., Manno, C., Henson, S. A., Tarling, G. A. and Sanders, R.: The role of particle associated
480 microbes in remineralization of fecal pellets in the upper mesopelagic of the Scotia Sea, Antarctica, *Limnol. Oceanogr.*,
481 61(3), 1049–1064, doi:10.1002/lno.10269, 2016b.

482 Besiktepe, S. and Dam, H. G.: Coupling of ingestion and defecation as a function of diet in the calanoid copepod *Acartia*
483 *tonsa*, *Mar. Ecol. Prog. Ser.*, 229(I), 151–164, doi:10.3354/meps229151, 2002.

484 Bodungen, von B., Fischer, G., Nothing, E. M. and Wefer, G.: Sedimentation of krill faeces during spring development of
485 phytoplankton in the Bransfield Strait, Antarctica, *Mitteilungen aus dem Geol. un Paläontologischen Inst. der Univ. Leipzig*,
486 62, 243–235, 1987.

487 Borrione, I. and Schlitzer, R.: Distribution and recurrence of phytoplankton blooms around South Georgia, Southern Ocean,
488 *Biogeosciences*, 10(1), 217–231, doi:10.5194/bg-10-217-2013, 2013.

489 Buesseler, K. O., Antia, A. N., Chen, M., Fowler, S. W., Gardner, W. D., Gustafsson, O., Harada, K., Michaels, A. F.,
490 Rutgers van der Loeff, M., Sarin, M., Steinberg, D. K. and Trull, T.: An assessment of the use of sediment traps for
491 estimating upper ocean particle fluxes, *J. Mar. Res.*, 65(3), 345–416, doi:10.1357/002224007781567621, 2007.

492 Butler, M. and Dam, H. G.: Production rates and characteristics of fecal pellets of the copepod *Acartia tonsa* under simulated
493 phytoplankton bloom conditions: implications for vertical fluxes, *Mar. Ecol. Prog. Ser.*, 114, 81–91,
494 doi:10.3354/meps114081, 1994.

495 Carroll, M. L., Miquel, J.-C. and Fowler, S. W.: Seasonal patterns and depth-specific trends of zooplankton fecal pellet
496 fluxes in the Northwestern Mediterranean Sea, *Deep Sea Res. Part I Oceanogr. Res. Pap.*, 45(8), 1303–1318,
497 doi:10.1016/S0967-0637(98)00013-2, 1998.

498 Cavan, E. L., Le Moigne, F., Poulton, A. J., Tarling, G. A., Ward, P., Daniels, C. J., G, F. and Sanders, R. J.: Attenuation of
499 particulate organic carbon flux in the Scotia Sea, Southern Ocean, controlled by zooplankton fecal pellets, *Geophys. Res.*
500 *Lett.*, 42(3), 821–830, doi:10.1002/2014GL062744, 2015.

501 Clarke, A., Quetin, L. B. and Ross, R. M.: Laboratory and field estimates of the rate of faecal pellet production by Antarctic
502 krill, *Euphausia superba*, *Mar. Biol.*, 98(4), 557–563, doi:10.1007/BF00391547, 1988.

503 Dagg, M. J., Urban-Rich, J. and Peterson, J. O.: The potential contribution of fecal pellets from large copepods to the flux of
504 biogenic silica and particulate organic carbon in the Antarctic Polar Front region near 170°W, *Deep Sea Res. Part II Top.*
505 *Stud. Oceanogr.*, 50(3–4), 675–691, doi:10.1016/S0967-0645(02)00590-8, 2003.

506 Daly, K. L.: Flux of particulate matter through copepods in the Northeast Water Polynya, *J. Mar. Syst.*, 10(1–4), 319–342,
507 doi:10.1016/S0924-7963(96)00062-0, 1997.

508 Engmann, S. and Cousineau, D.: Comparing distributions: The two-sample Anderson-Darling test as an alternative to the

509 Kolmogorov-Smirnoff test, *J. Appl. Quant. methods*, 6(3), 1–17, 2011.

510 Fowler, S. W., Small, L. F. and La Rosa, J.: Seasonal particulate carbon flux in the coastal northwestern Mediterranean Sea ,
511 and the role of zooplankton fecal matter, *Oceanol. Acta*, 14(1), 77–85, 1991.

512 Gleiber, M. R., Steinberg, D. K. and Ducklow, H. W.: Time series of vertical flux of zooplankton fecal pellets on the
513 continental shelf of the western Antarctic Peninsula, *Mar. Ecol. Prog. Ser.*, 471, 23–36, doi:10.3354/meps10021, 2012.

514 González, H. E.: The distribution and abundance of krill faecal material and oval pellets in the Scotia and Weddell Seas
515 (Antarctica) and their role in particle flux, *Polar Biol.*, 12, 81–91, doi:10.1007/BF00239968, 1992.

516 González, H. E. and Smetacek, V.: The possible role of the cyclopoid copepod *Oithona* in retarding vertical flux of
517 zooplankton faecal material, *Mar. Ecol. Prog. Ser.*, 113(1982), 233–246, 1994.

518 González, H. E., Kurbjeweit, F. and Bathmann, U. V: Occurrence of cyclopoid copepods and faecal material in the Halley
519 Bay region, Antarctica, during January-February 1991, *Polar Biol.*, 14(5), 331–342, doi:10.1007/BF00238449, 1994a.

520 González, H. E., González, S. R. and Brummer, G. A.: Short-term sedimentation pattern of zooplankton, faeces and
521 microplankton at a permanent station in the Bjarnafjorden (Norway) during April-May 1992, *Mar. Ecol. Prog. Ser.*, 105, 31–
522 45, 1994b.

523 Hamm, C., Reigstad, M., Riser, C. W., Mühlebach, A. and Wassmann, P.: On the trophic fate of *Phaeocystis pouchetii*. VII.
524 Sterols and fatty acids reveal sedimentation of *P. pouchetii*-derived organic matter via krill fecal strings, *Mar Ecol Prog Ser*,
525 209, 55–69, doi:10.3354/meps209055, 2001.

526 Head, E. J. H.: Comparison of the chemical composition of particulate material and copepod faecal pellets at stations off the
527 coast of Labrador and in the Gulf of St. Lawrence, *Mar. Biol.*, 112(4), 593–600, doi:10.1007/BF00346177, 1992.

528 Iversen, M. H. and Poulsen, L.: Coprorhexy, coprophagy, and coprochaly in the copepods *Calanus helgolandicus*,
529 *Pseudocalanus elongatus*, and *Oithona similis*, *Mar. Ecol. Prog. Ser.*, 350(1990), 79–89, doi:10.3354/meps07095, 2007.

530 Jónasdóttir, S. H., Visser, A. W., Richardson, K. and Heath, M. R.: Seasonal copepod lipid pump promotes carbon
531 sequestration in the deep North Atlantic., *Proc. Natl. Acad. Sci. U. S. A.*, 112(39), 12122–6, doi:10.1073/pnas.1512110112,
532 2015.

533 Kobari, T., Steinberg, D. K., Ueda, A., Tsuda, A., Silver, M. W. and Kitamura, M.: Impacts of ontogenetically migrating
534 copepods on downward carbon flux in the western subarctic Pacific Ocean, *Deep Sea Res. Part II Top. Stud. Oceanogr.*,
535 55(14–15), 1648–1660, doi:10.1016/j.dsr2.2008.04.016, 2008.

536 Komar, P. D., Morse, A. P., Small, L. F. and Fowler, S. W.: An analysis of sinking rates of natural copepod and euphausiid
537 fecal pellets, *Limnol. Oceanogr.*, 26, 172–180, doi:10.4319/lo.1981.26.1.0172, 1981.

538 Korb, R. E., Whitehouse, M. J., Atkinson, A. and Thorpe, S.: Magnitude and maintenance of the phytoplankton bloom at
539 South Georgia: a naturally iron-replete environment, *Mar. Ecol. Prog. Ser.*, 368, 75–91, doi:10.3354/meps07525, 2008.

540 Korb, R. E., Whitehouse, M. J., Ward, P., Gordon, M., Venables, H. J. and Poulton, A. J.: Regional and seasonal differences
541 in microplankton biomass, productivity, and structure across the Scotia Sea: Implications for the export of biogenic carbon,
542 *Deep Sea Res. Part II Top. Stud. Oceanogr.*, 59–60, 67–77, doi:10.1016/j.dsr2.2011.06.006, 2012.

543 Kwon, E. Y., Primeau, F. and Sarmiento, J. L.: The impact of remineralization depth on the air–sea carbon balance, *Nat.*
544 *Geosci.*, 2(9), 630–635, doi:10.1038/ngeo612, 2009.

545 Laakmann, S., Stumpp, M. and Auel, H.: Vertical distribution and dietary preferences of deep-sea copepods (Euchaetidae
546 and Aetideidae; Calanoida) in the vicinity of the Antarctic Polar Front, *Polar Biol.*, 32(5), 679–689, doi:10.1007/s00300-
547 008-0573-2, 2009.

548 Lampitt, R. S., Noji, T. and Bodungen, B. Von: What happens to zooplankton faecal pellets? Implications for material flux,
549 *Mar. Biol.*, 104, 15–23, doi:10.1007/BF01313152, 1990.

550 Manno, C., Stowasser, G., Enderlein, P., Fielding, S. and Tarling, G. A.: The contribution of zooplankton faecal pellets to
551 deep-carbon transport in the Scotia Sea (Southern Ocean), *Biogeosciences*, 12(6), 1955–1965, doi:10.5194/bg-12-1955-
552 2015, 2015.

553 Martens, P.: Faecal pellets, *Fich. Ident. Zooplankt.*, 162, 1–4, 1978.

554 Martin, J. H., Knauer, G. A., Karl, D. M. and Broenkow, W. W.: VERTEX: carbon cycling in the northeast Pacific, *Deep*
555 *Sea Res. Part I Oceanogr. Res. Pap.*, 34(2), 267–285, doi:10.1016/0198-0149(87)90086-0, 1987.

556 Mauchline, J.: The biology of calanoid copepods, *Adv. Mar. Biol.*, 33, 710, 1998.

557 Miquel, J.-C., Gasser, B., Martín, J., Marec, C., Babin, M., Fortier, L. and Forest, A.: Downward particle flux and carbon
558 export in the Beaufort Sea, Arctic Ocean; the role of zooplankton, *Biogeosciences*, 12(16), 5103–5117, doi:10.5194/bg-12-
559 5103-2015, 2015.

560 Murphy, E. J., Watkins, J. L., Trathan, P. N., Reid, K., Meredith, M. P., Thorpe, S. E., Johnston, N. M., Clarke, A., Tarling,
561 G. A., Collins, M. A., Forcada, J., Shreeve, R. S., Atkinson, A., Korb, R., Whitehouse, M. J., Ward, P., Rodhouse, P. G.,
562 Enderlein, P., Hirst, A. G., Martin, A. R., Hill, S. L., Staniland, I. J., Pond, D. W., Briggs, D. R., Cunningham, N. J. and
563 Fleming, A. H.: Spatial and temporal operation of the Scotia Sea ecosystem: a review of large-scale links in a krill centred
564 food web, *Philos. Trans. R. Soc. B Biol. Sci.*, 362(1477), 113–148, doi:10.1098/rstb.2006.1957, 2007.

565 Orsi, H., Whitworth III, T. and Nowlin Jr, W. D.: On the meridional extent and fronts of the Antarctic Circumpolar Current,
566 *Deep Sea Res. Part I Oceanogr. Res. Pap.*, 42(5), 641–673, doi:10.1016/0967-0637(95)00021-W, 1995.

567 Parekh, P., Dutkiewicz, S., Follows, M. J. and Ito, T.: Atmospheric carbon dioxide in a less dusty world, *Geophys. Res.*
568 *Lett.*, 33(3), L03610, doi:10.1029/2005GL025098, 2006.

569 Park, J., Oh, I.-S., Kim, H.-C. and Yoo, S.: Variability of SeaWiFs chlorophyll-a in the southwest Atlantic sector of the
570 Southern Ocean: Strong topographic effects and weak seasonality, *Deep Sea Res. Part I Oceanogr. Res. Pap.*, 57(4), 604–
571 620, doi:10.1016/j.dsr.2010.01.004, 2010.

572 Ploug, H. and Jorgensen, B. B.: A net-jet flow system for mass transfer and microsensor studies of sinking aggregates, *Mar.*
573 *Ecol. Prog. Ser.*, 176(1987), 279–290, doi:10.3354/meps176279, 1999.

574 Poulsen, L. and Iversen, M. H.: Degradation of copepod fecal pellets: key role of protozooplankton, *Mar. Ecol. Prog. Ser.*,
575 367, 1–13, doi:10.3354/meps07611, 2008.

576 Poulsen, L. and Kiørboe, T.: Coprophagy and coprorhexy in the copepods *Acartia tonsa* and *Temora longicornis*: clearance

577 rates and feeding behaviour, *Mar. Ecol. Prog. Ser.*, 299, 217–227, doi:10.3354/meps299217, 2005.

578 Reigstad, M., Riser, C. W. and Svensen, C.: Fate of copepod faecal pellets and the role of *Oithona* spp., *Mar. Ecol. Prog.*
579 *Ser.*, 304, 265–270, 2005.

580 Riley, J. S., Sanders, R., Marsay, C., Le Moigne, F., Achterberg, E. P. and Poulton, A. J.: The relative contribution of fast
581 and slow sinking particles to ocean carbon export, *Global Biogeochem. Cycles*, 26, doi:10.1029/2011GB004085, 2012.

582 Roy, S., Silverberg, N., Romero, N., Deibel, D., Klein, B., Savenkoff, C., V??zina, A., Tremblay, J. ??, Legendre, L. and
583 Rivkin, R. B.: Importance of mesozooplankton feeding for the downward flux of biogenic carbon in the Gulf of St.
584 Lawrence (Canada), *Deep. Res. Part II Top. Stud. Oceanogr.*, 47(3–4), 519–544, doi:10.1016/S0967-0645(99)00117-4,
585 2000.

586 Sarmiento, J. L. and Gruber, N.: *Ocean Biogeochemical Dynamics*, Princeton University Press, Princeton., 2006.

587 Small, L. F., Fowler, S. W. and Ünlü, M. Y.: Sinking rates of natural copepod fecal pellets, *Mar. Biol.*, 51(3), 233–241,
588 doi:10.1007/BF00386803, 1979.

589 Smetacek, V., Assmy, P. and Henjes, J.: The role of grazing in structuring Southern Ocean pelagic ecosystems and
590 biogeochemical cycles, *Antarct. Sci.*, 16(4), 541–558, doi:10.1017/S0954102004002317, 2004.

591 Smith, Jr., K. L., Sherman, A. D., Huffard, C. L., McGill, P. R., Henthorn, R., Von Thun, S., Ruhl, H. A., Kahru, M. and
592 Ohman, M. D.: Large salp bloom export from the upper ocean and benthic community response in the abyssal northeast
593 Pacific: Day to week resolution, *Limnol. Oceanogr.*, 59(3), 745–757, doi:10.4319/lo.2014.59.3.0745, 2014.

594 Stamieszkin, K., Pershing, A. J., Record, N. R., Pilskalns, C. H., Dam, H. G. and Feinberg, L. R.: Size as the master trait in
595 modeled copepod fecal pellet carbon flux, *Limnol. Oceanogr.*, 60, 2090–2107, doi:10.1002/lno.10156, 2015.

596 Steinberg, D. K., Carlson, C. A., Bates, N. R., Goldthwait, S. A., Madin, L. P. and Michaels, A. F.: Zooplankton vertical
597 migration and the active transport of dissolved organic and inorganic carbon in the Sargasso Sea, *Deep Sea Res. Part I*
598 *Oceanogr. Res. Pap.*, 47, 137–158, doi:10.1016/S0967-0637(99)00052-7, 2000.

599 Suzuki, H., Sasaki, H. and Fukuchi, M.: Short-term variability in the flux of rapidly sinking particles in the Antarctic
600 marginal ice zone, *Polar Biol.*, 24(9), 697–705, doi:10.1007/s003000100271, 2001.

601 Suzuki, H., Sasaki, H. and Fukuchi, M.: Loss processes of sinking fecal pellets of zooplankton in the mesopelagic layers of
602 the Antarctic marginal ice zone, *J. Oceanogr.*, 59(6), 809–818, doi:10.1023/B:JOCE.0000009572.08048.0d, 2003.

603 Svensen, C. and Nejstgaard, J. C.: Is sedimentation of copepod faecal pellets determined by cyclopoids? Evidence from
604 enclosed ecosystems, *J. Plankton Res.*, 25(8), 917–926, doi:10.1093/plankt/25.8.917, 2003.

605 Thibault, D., Roy, S., Wong, C. S. and Bishop, J. K.: The downward flux of biogenic material in the NE subarctic Pacific:
606 Importance of algal sinking and mesozooplankton herbivory, *Deep. Res. Part II Top. Stud. Oceanogr.*, 46(11–12), 2669–
607 2697, doi:10.1016/S0967-0645(99)00080-6, 1999.

608 Thorpe, S. E., Heywood, K. J., Brandon, M. A. and Stevens, D. P.: Variability of the southern Antarctic Circumpolar Current
609 front north of South Georgia, *J. Mar. Syst.*, 37(1–3), 87–105, doi:10.1016/S0924-7963(02)00197-5, 2002.

610 Thorpe, S. E., Murphy, E. J. and Watkins, J. L.: Circumpolar connections between Antarctic krill (*Euphausia superba* Dana)

611 populations: investigating the roles of ocean and sea ice transport, *Deep Sea Res. Part A. Oceanogr. Res. Pap.*, 54, 794–810,
612 doi:10.1016/j.dsr.2007.01.008, 2007.

613 Turner, J. T.: Zooplankton fecal pellets, marine snow and sinking phytoplankton blooms, *Aquat. Microb. Ecol.*, 27, 57–102,
614 doi:doi:10.3354/ame027057, 2002.

615 Turner, J. T.: Zooplankton fecal pellets, marine snow, phytodetritus and the ocean's biological pump, *Prog. Oceanogr.*, 130,
616 205–248, doi:10.1016/j.pocean.2014.08.005, 2015.

617 Urban-Rich, J., Nordby, E. and Andreassen, I.: Contribution by mezooplankton focal pellets to the carbon flux on
618 Nordvestkbanken, north Norwegian shelf in 1994, *Sarsia*, 84(March), 253–264, doi:10.1080/00364827.1999.10420430,
619 1999.

620 Urrere, M. A. and Knauer, G. A.: Zooplankton fecal pellet fluxes and vertical transport of particulate organic material in the
621 pelagic environment, *J. Plankton Res.*, 3(3), 369–387, doi:10.1093/plankt/3.3.369, 1981.

622 Viitasalo, M., Rosenberg, M., Heiskanen, A.-S. and Koski, M.: Sedimentation of copepod fecal material in the coastal
623 northern Baltic Sea: Where did all the pellets go?, *Limnol. Ocean.*, 44(6), 1388–1399, doi:10.4319/lo.1999.44.6.1388, 1999.

624 Vinogradov, M. E.: Feeding of the deep-sea zooplankton, *Rapp P- V Cons. Int. Explor. Mer*, 153, 114–120, 1962.

625 Volk, T. and Hoffert, M. I.: Ocean Carbon Pumps: Analysis of relative strengths and efficiencies in ocean driven
626 atmospheric CO₂ changes, in *The carbon cycle and atmospheric CO₂: Natural variations Archean to Present*, edited by E. T.
627 Sundquist and W. S. Broecker, pp. 99–110, American Geophysical Union, Washington, DC., 1985.

628 Wallace, M. I., Cottier, F. R., Brierley, A. S. and Tarling, G. A.: Modelling the influence of copepod behaviour on faecal
629 pellet export at high latitudes, *Polar Biol.*, 36(4), 579–592, doi:10.1007/s00300-013-1287-7, 2013.

630 Ward, P. and Shreeve, R.: The spring mesozooplankton community at South Georgia: a comparison of shelf and oceanic
631 sites, *Polar Biol.*, 22, 289–301, doi:10.1007/s003000050422, 1999.

632 Ward, P., Atkinson, A., Murray, A. W. A., Wood, A. G., Williams, R. and Poulet, S. A.: The summer zooplankton
633 community at South Georgia: biomass, vertical migration and grazing, *Polar Biol.*, 195–208, doi:10.1007/BF00239059,
634 1995.

635 Ward, P., Shreeve, R., Atkinson, A., Korb, B., Whitehouse, M., Thorpe, S., Pond, D. and Cunningham, N.: Plankton
636 community structure and variability in the Scotia Sea: austral summer 2003, *Mar. Ecol. Prog. Ser.*, 309, 75–91,
637 doi:10.3354/meps309075, 2006a.

638 Ward, P., Shreeve, R. and Tarling, G. A.: The autumn mesozooplankton community at South Georgia: Biomass, population
639 structure and vertical distribution, *Polar Biol.*, 29(11), 950–962, doi:10.1007/s00300-006-0136-3, 2006b.

640 Ward, P., Atkinson, A. and Tarling, G.: Mesozooplankton community structure and variability in the Scotia Sea: A seasonal
641 comparison, *Deep Sea Res. Part II Top. Stud. Oceanogr.*, 59–60, 78–92, doi:10.1016/j.dsr2.2011.07.004, 2012.

642 Ward, P., Tarling, G. A. and Thorpe, S. E.: Mesozooplankton in the Southern Ocean: Spatial and temporal patterns from
643 Discovery Investigations, *Prog. Oceanogr.*, 120, 305–319, doi:10.1016/j.pocean.2013.10.011, 2014.

644 Wassmann, P., Erik, J. and Tselepidis, A.: Vertical flux of faecal pellets and microplankton on the shelf of the oligotrophic

645 Cretan Sea (NE Mediterranean Sea), *Prog. Oceanogr.*, 46, 241–258, doi:10.1016/S0079-6611(00)00021-5, 2000.

646 Wexels-Riser, C., Wassmann, P., Olli, K. and Arashkevich, E.: Production, retention and export of zooplankton faecal
647 pellets on and off the Iberian shelf, north-west Spain, *Prog. Oceanogr.*, 51(2–4), 423–441, doi:10.1016/S0079-
648 6611(01)00078-7, 2001.

649 Wexels Riser, C., Reigstad, M., Wassmann, P., Arashkevich, E. and Falk-Petersen, S.: Export or retention? Copepod
650 abundance, faecal pellet production and vertical flux in the marginal ice zone through snap shots from the northern Barents
651 Sea, *Polar Biol.*, 30, 719–730, doi:10.1007/s00300-006-0229-z, 2007.

652 Wexels Riser, C., Reigstad, M. and Wassmann, P.: Zooplankton-mediated carbon export : A seasonal study in a northern
653 Norwegian fjord Norwegian fjord, *Mar. Biol. Res.*, 6(5), 461–471, doi:10.1080/17451000903437067, 2010.

654 Whitehouse, M. J., Korb, R. E., Atkinson, A., Thorpe, S. E. and Gordon, M.: Formation, transport and decay of an intense
655 phytoplankton bloom within the High-Nutrient Low-Chlorophyll belt of the Southern Ocean, *J. Mar. Syst.*, 70(1–2), 150–
656 167, doi:10.1016/j.jmarsys.2007.05.003, 2008.

657 Whitehouse, M. J., Atkinson, A., Korb, R. E., Venables, H. J., Pond, D. W. and Gordon, M.: Substantial primary production
658 in the land-remote region of the central and northern Scotia Sea, *Deep Sea Res. Part II Top. Stud. Oceanogr.*, 59–60, 47–56,
659 doi:10.1016/j.dsr2.2011.05.010, 2012.

660 Wilson, S. E., Steinberg, D. K. and Buesseler, K. O.: Changes in fecal pellet characteristics with depth as indicators of
661 zooplankton repackaging of particles in the mesopelagic zone of the subtropical and subarctic North Pacific Ocean, *Deep
662 Sea Res. Part II Top. Stud. Oceanogr.*, 55(14–15), 1636–1647, doi:10.1016/j.dsr2.2008.04.019, 2008.

663 Wilson, S. E., Ruhl, H. A. and Smith, K. L.: Zooplankton fecal pellet flux in the abyssal northeast Pacific : A 15 year time-
664 series study, *Limnol. Oceanogr.*, 58(3), 881–892, doi:10.4319/lo.2013.58.3.0881, 2013.

665 Yoon, W. D., Kim, S. K. and Han, K. N.: Morphology and sinking velocities of fecal pellets of copepod, molluscan,
666 euphausiid, and salp taxa in the northeastern tropical Atlantic, *Mar. Biol.*, 139(5), 923–928, doi:10.1007/s002270100630,
667 2001.

668

669

671 **Table 1: Details of marine snow catcher (MSC) deployments during cruises JR291 and JR304 to the Scotia Sea**

Cruise	Site	Latitude	Longitude	Date	Time (GMT)	Depth of MSC (m)
JR291	P2	-55.192	-41.342	02/12/2013	23:45	176
	P2	-55.196	-41.332	03/12/2013	15:54	204
	P2	-55.259	-41.295	07/12/2013	15:07	203
	P3	-52.769	-40.155	13/12/2013	13:49	205
	P3	-52.769	-40.154	14/12/2013	06:33	180
JR304	P3	-52.8116	-39.9727	12/12/2014	22:40	176
	P3	-52.8118	-39.9726	13/12/2014	22:47	183

672

673

674 **Table 2: FP fluxes (\pm SE, nFP $m^{-2} d^{-1}$) of ovoid, cylindrical and elliptical (Cyl+Ell), and round FP at P2 and P3 as measured in**
675 **Marine Snow Catchers (MSC) and sediment traps (ST) in the Scotia Sea in spring.**

	P2				P3			
	Ovoid	Cyl + Ell	Round	Total	Ovoid	Cyl + Ell	Round	Total
MSC	6,309 (\pm 2,698)	21,128 (\pm 1,328)	14,596 (\pm 1,124)	89,850 (\pm 11,922)	13,416 (\pm 8,207)	190,716 (\pm 51,623)	32,172 (\pm 15,239)	236,304 (\pm 63,079)
ST	640 (\pm 33)	238 (\pm 82)	175 (\pm 37)	1,052 (\pm 152)	11,226 (\pm 706)	7,406 (\pm 1,274)	4,668 (\pm 14)	23,300 (\pm 1,994)
MSC/ST	9.9	88.9	83.5	39.9	1.2	25.8	6.9	10.1

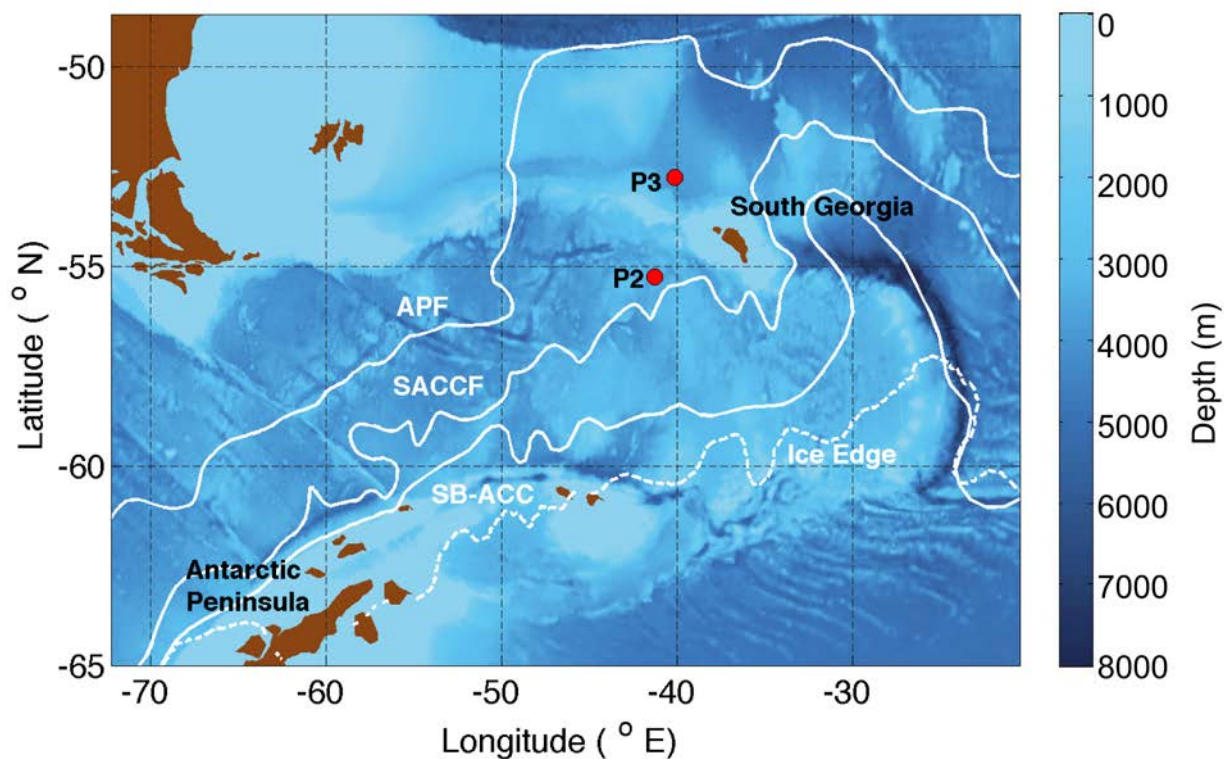
676

677

678 **Figures and Figure Legends**

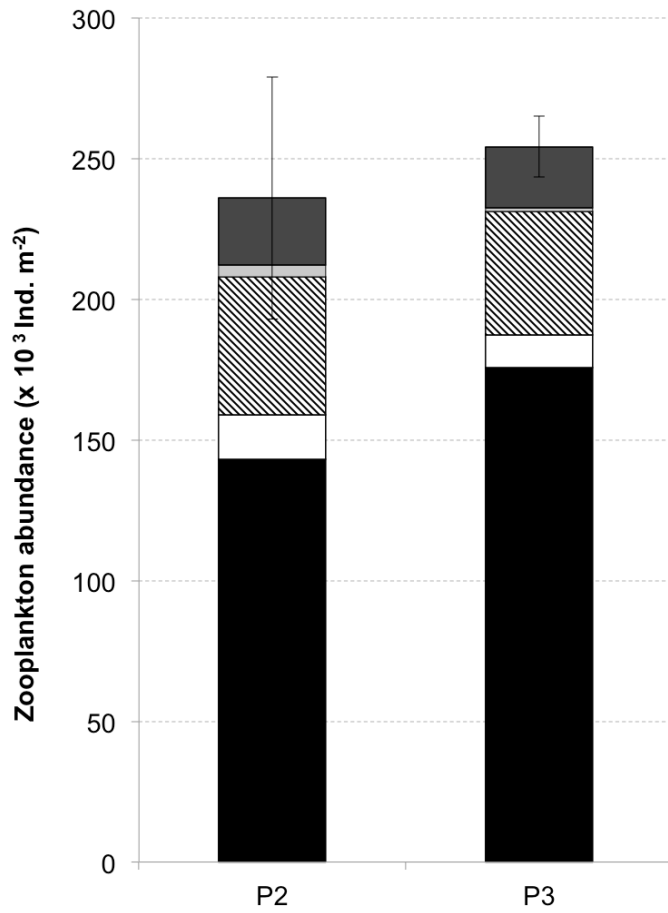
679

680



681

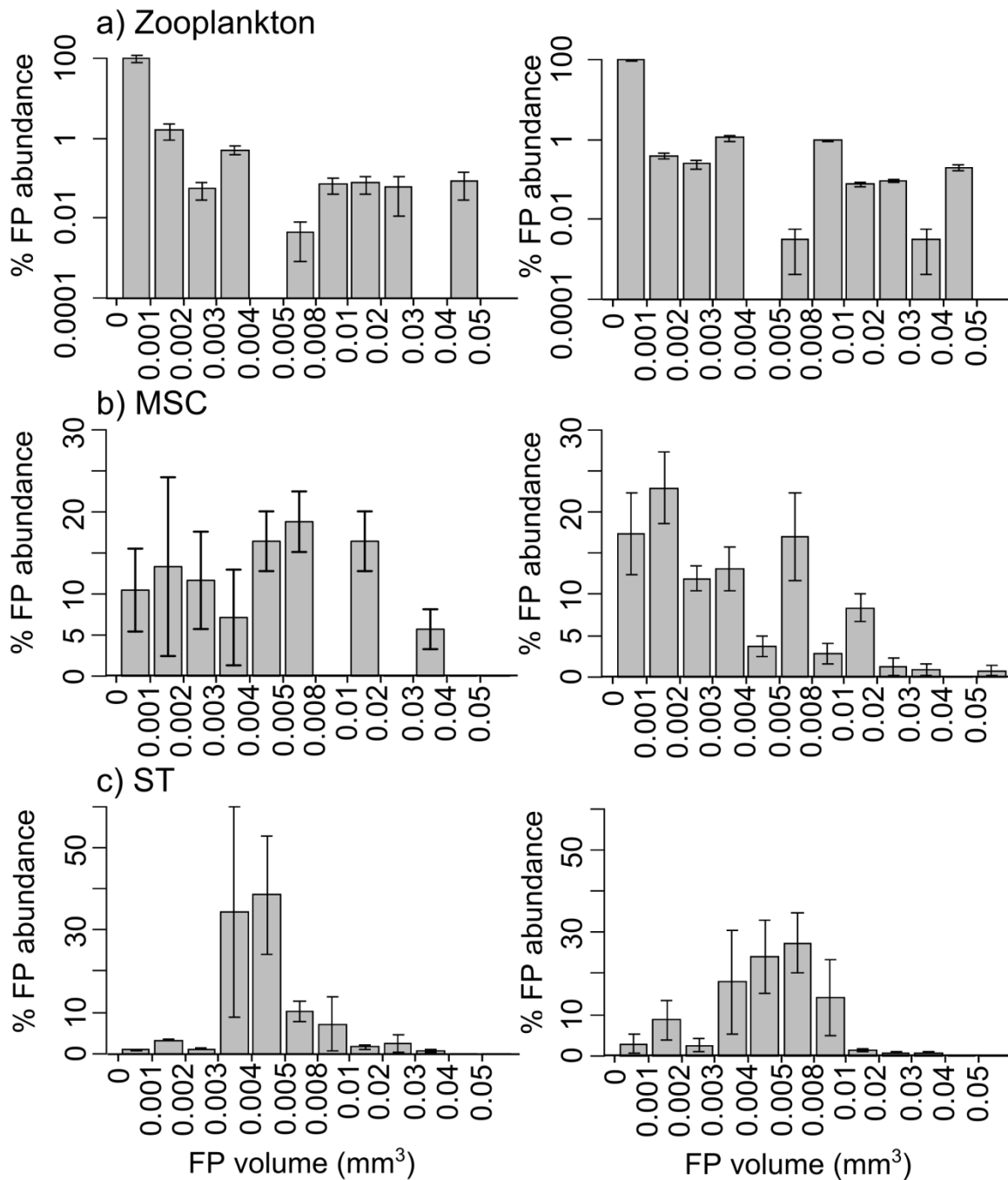
682 **Figure 1: Stations sampled in the Scotia Sea. White lines indicate average frontal positions. APF=Antarctic Polar Front (Orsi et al.,**
683 **SACCF = Southern Antarctic Circumpolar Current Front (Thorpe et al., 2002), SB-ACC=Southern Boundary - Antarctic**
684 **Circumpolar Current (Orsi et al., 1995). White dotted lines indicates the position of the ice edge on 3rd Dec 2013 (OSTIA Sea Ice**
685 **satellite data).**



686

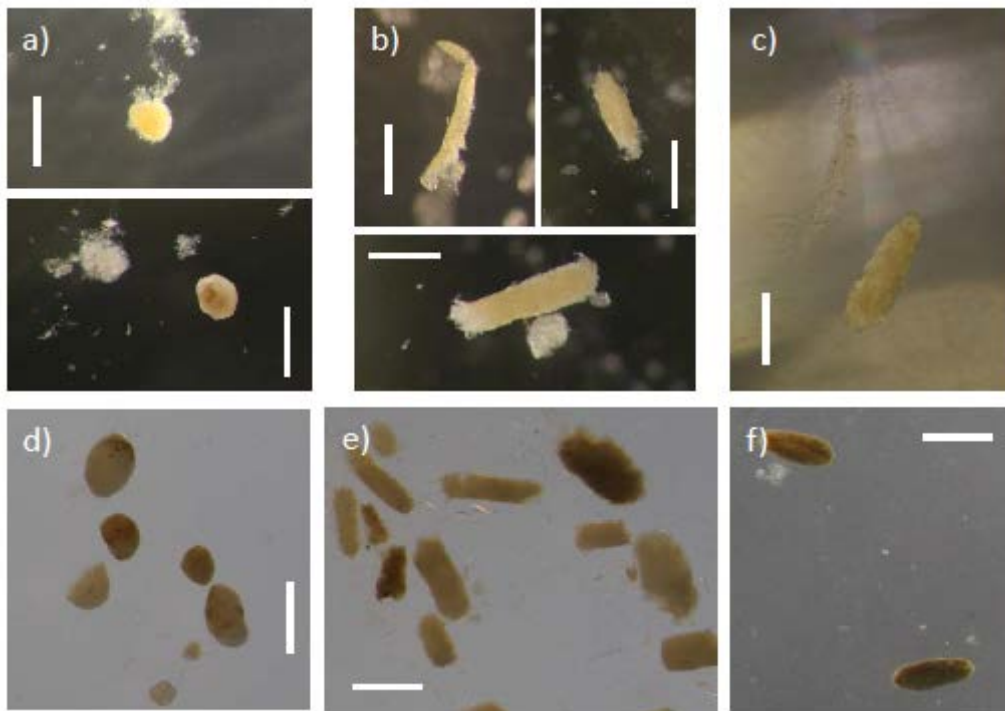
687 **Figure 2: Average zooplankton abundances ($\times 10^3$ Ind. m^{-2} (0-200m)) measured in the Scotia Sea in December 2013 and 2014**
 688 **using a 200 μm mesh. Small microcopepods (black), large calanoids (white), other copepods (striped), small euphausiids (light**
 689 **grey), other zooplankton (dark grey) (see text for full details on groups). Error bars show \pm SE of total zooplankton abundance**
 690 **based on multiple Bongo net tows at each site.**

691



692

693 **Figure 3: Faecal pellet size distributions for P2 (left) and P3 (right) in the Scotia Sea. The percent (%) abundance of faecal pellets**
 694 **in each size class (volume, mm³) is presented for; a) estimated egested faecal pellet size distributions based on mesozooplankton**
 695 **abundances (200 μ m mesh), b) faecal pellets measured in marine snow catchers (MSC) at MLD+110 m averages (\pm SE), and c)**
 696 **faecal pellets in sediment traps (ST). Krill faecal pellets have been removed. Note the uneven faecal pellet volume size classes, and**
 697 **log scale on the Y axis for a.**



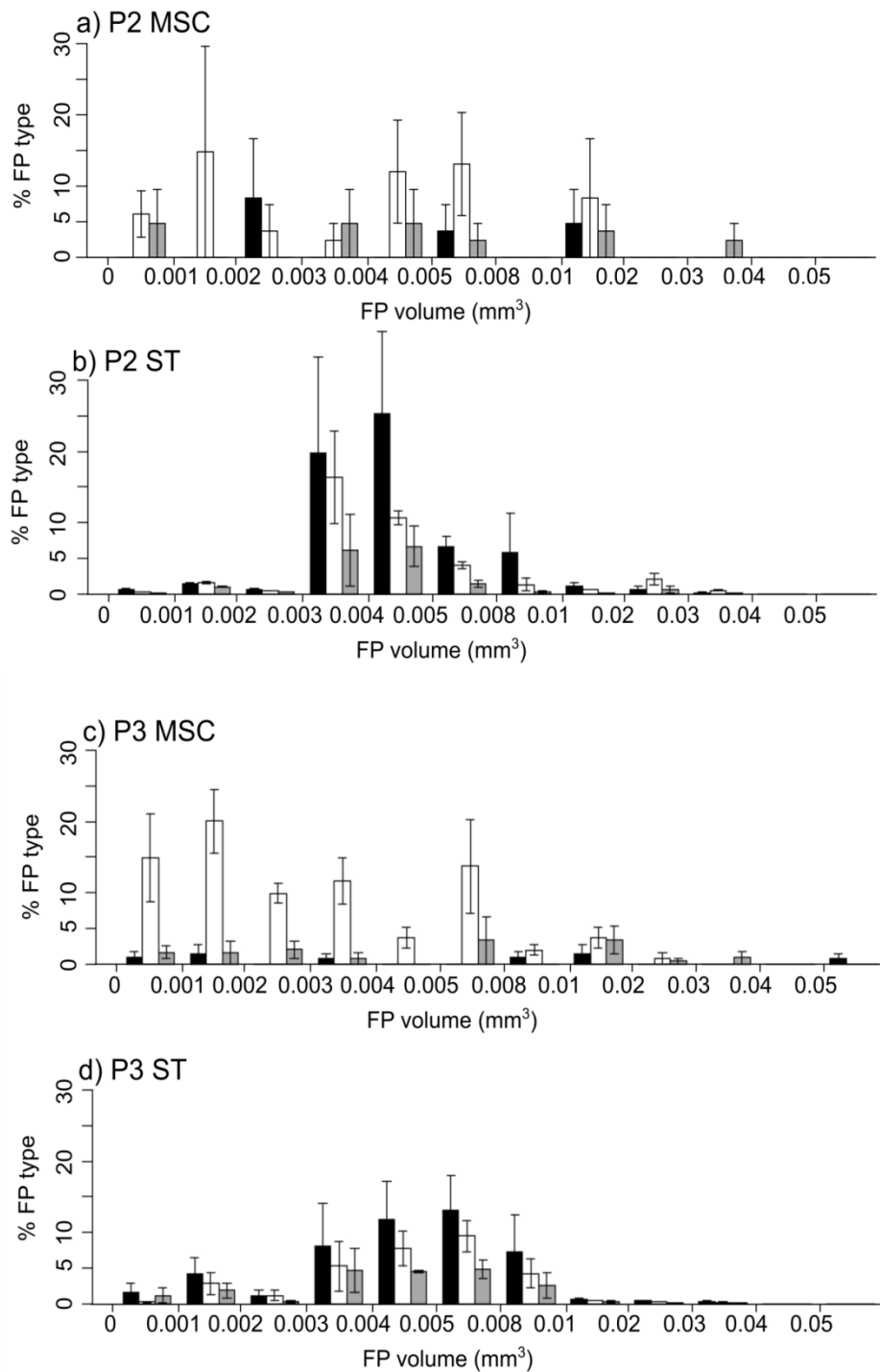
698

699

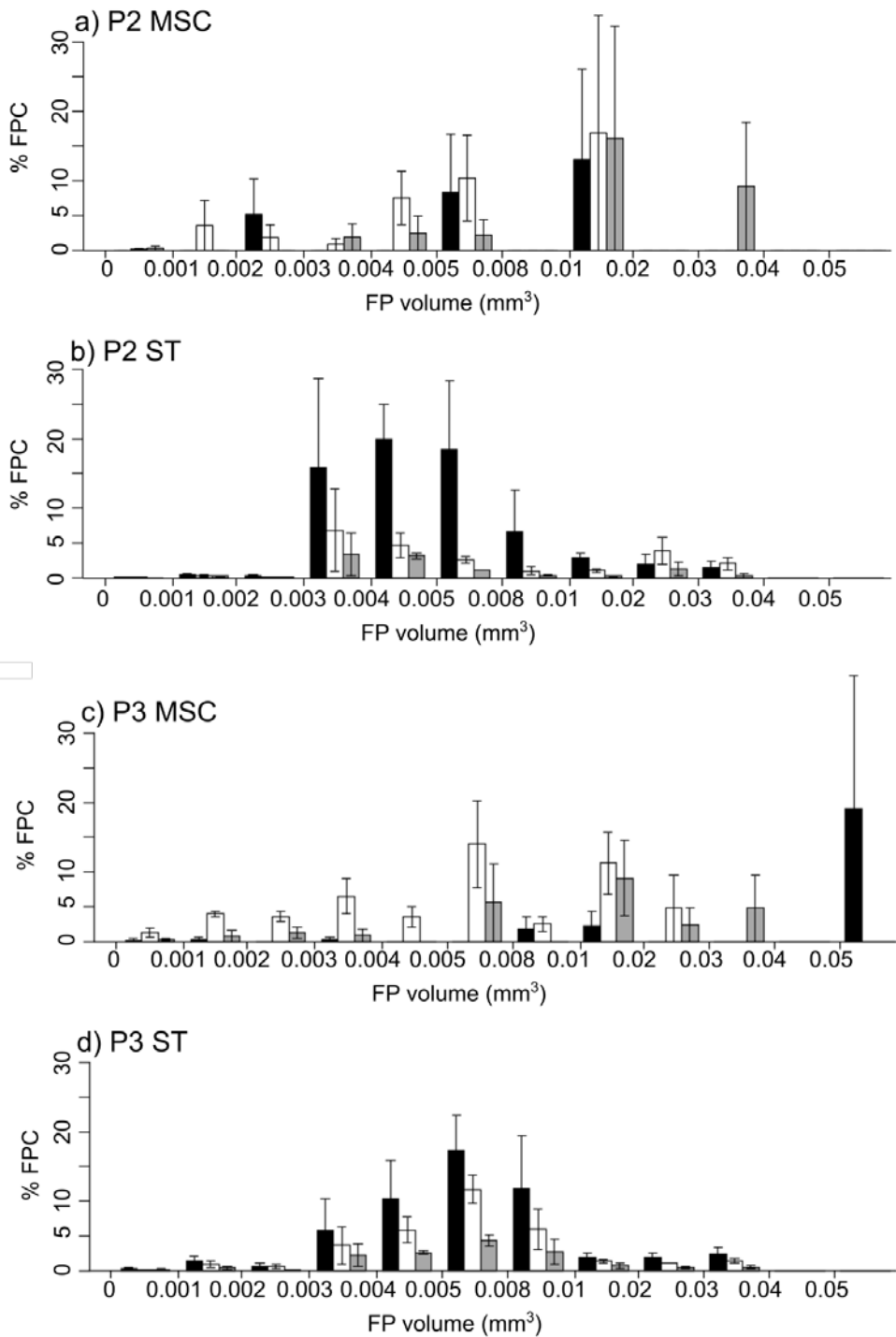
700

Figure 4: Light microscopy photographs of faecal pellets collected from Marine Snow Catchers (A-C) and sediment traps (D-F). The different morphological classes are illustrated; a)+d)) round, b)+e) cylindrical, c)+f) ovoid. Scale bar = 0.5 mm.

701



702 **Figure 5:** Percent (%) contribution of each pellet type to total faecal pellet abundance, ovoid (black), cylindrical and elliptical
 703 (white) and round (grey). FP from a) P2 Marine Snow Catcher, b) P2 sediment trap, c) P3 Marine Snow Catcher, d) P3 sediment
 704 trap. Krill faecal pellets have been removed. Note the uneven faecal pellet volume size classes.
 705



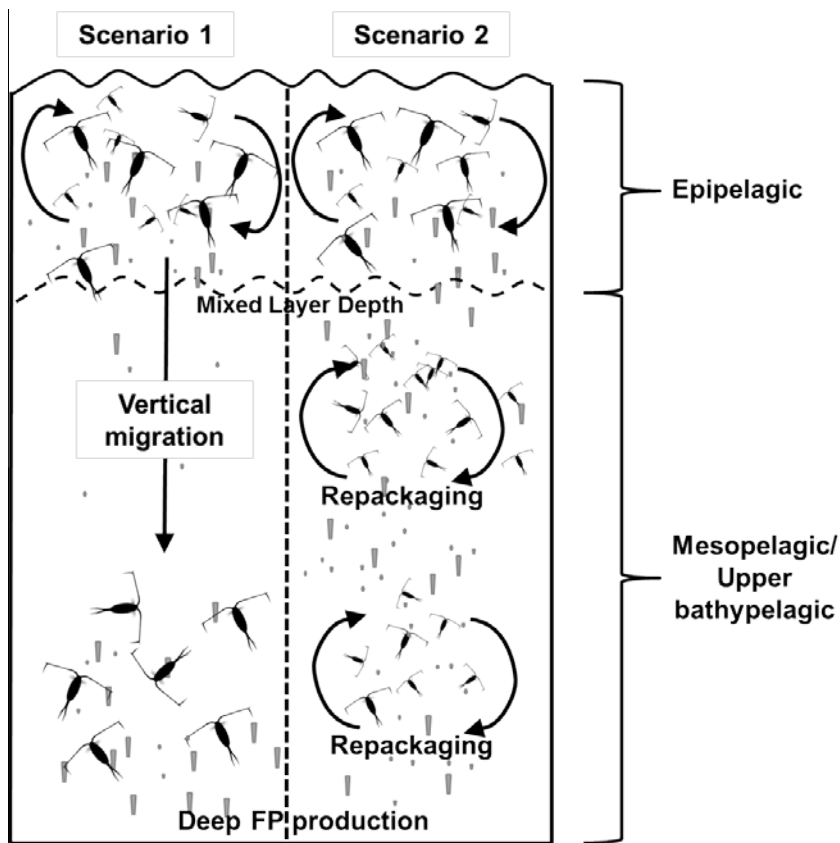
706

707

708

709

Figure 6: Percent (%) contribution of each pellet type to total faecal pellet carbon, ovoid (black), cylindrical and elliptical (white) and round (grey). FP from a) P2 Marine Snow Catcher, b) P2 sediment trap, c) P3 Marine Snow Catcher, d) P3 sediment trap. Krill faecal pellets have been removed. Note the uneven faecal pellet volume size classes.



710
711
712
713
714

Figure 7: Schematic to illustrate the possible mechanisms of deep FP production that are suggested to be occurring at our study sites in the Scotia Sea. In Scenario 1, intact FP reach the deep ocean via vertical migration of zooplankton whereas, in Scenario 2, FP at depth result from in situ repackaging of sinking detritus by deep dwelling zooplankton. The actual mechanisms occurring in the mesopelagic are likely to be a complex combination of both scenarios.

715

716 **Supplementary Table**

717 **Table S1: Absolute number of FP counted in sediment trap (ST) sample split and Marine Snow Catcher (MSC) samples. Three**
 718 **replicates were counted for ST samples and are presented as mean (standard deviation), where as all FP collected in the MSC**
 719 **samples were counted. Krill FP are not included.**

Cruise	Site	Sampling Method	# FP
JR291	P2	MSC	4
	P2	MSC	9
	P2	MSC	28
	P3	MSC	15
	P3	MSC	74
JR304	P3	MSC	120
	P3	MSC	252
Dec 2009	P2	ST	422 (98)
	P3	ST	1156 (195)
Dec 2010	P2	ST	564 (134)
	P3	ST	974 (238)

720

721 **Table S2: Sinking velocities and volumes of FP (excluding krill FP) collected in Marine Snow Catchers at P2 and P3 during**
 722 **research cruises JR291 and JR304.**

Site	FP volume (mm ³)	FP sinking velocity (m d ⁻¹)	Site	FP volume (mm ³)	FP sinking velocity (m d ⁻¹)
P2	0.040	144	P3	0.010	75
P2	0.031	270	P3	0.027	57
P2	0.008	52	P3	0.002	48
P2	0.040	144	P3	0.026	87
P2	0.031	135	P3	0.002	51
P2	0.057	134	P3	0.005	68
P2	0.019	342	P3	0.014	49
P2	0.011	382	P3	0.028	92
P2	0.072	247	P3	0.023	106
P2	0.044	101	P3	0.009	24
P2	0.007	193	P3	0.091	92
P2	0.017	116	P3	0.066	140
P2	0.035	207	P3	0.012	57
P2	0.002	246	P3	0.006	65
P2	0.016	61	P3	0.010	62
P2	0.001	120	P3	0.006	64

P2	0.003	98	P3	0.002	47
			P3	0.037	36
			P3	0.031	53
			P3	0.014	122
			P3	0.021	36
			P3	0.077	100
			P3	0.018	62
			P3	0.026	64
			P3	0.013	79
			P3	0.083	227
			P3	0.286	203
			P3	0.165	189
			P3	0.007	100
			P3	0.006	74
			P3	0.005	13
			P3	0.115	106
			P3	0.021	60
			P3	0.005	68
			P3	0.018	79
			P3	0.006	49
			P3	0.009	64
			P3	0.003	155
			P3	0.005	222
			P3	0.256	144
			P3	0.002	82
			P3	0.006	133
